Monocyclopentadienyl Pentafluorothiophenolate Complexes of Molybdenum and Their Interactions with Thallium(I) Ions; Dynamic Nuclear Magnetic Resonance Studies and Crystal and Molecular Structures of [TlMo(SC6F5)2L2(cp)] (L = CO or SC6F5; cp = η5-C5H5)†

W. A. Wan Abu Bakar, Jack L. Davidson,* W. Edward Lindsell,* and Kevin J. McCullough*
Department of Chemistry, Heriot-Watt University, Riccarton, Edinburgh EH14 4AS
Kenneth W. Muir
Department of Chemistry, University of Glasgow, Glasgow G12 8QQ

Reactions between [MoCl(CO)3(cp)] (cp = η5-C5H5) and Tl(SC6F5) afford the fully characterised complexes [TlMo(SC6F5)2L2(cp)] [L = CO (**1**) or SC6F5 (**2**)]. Complex (**2**) is formed by an oxidative substitution process and can also be obtained by reactions of Tl(SC6F5) with other molybdenum-(II), -(III), or -(IV) precursors. Molecular structures of crystalline complexes (**1**) and (**2**) have been determined by X-ray diffraction. Complex (**1**) contains units of [(cp)(OC)2Mo(μ-SC6F5)2Tl] in which Tl^I is co-ordinated by two S atoms (mean Tl–S 3.015 Å) and is close to one *ortho*-F atom of each C6F5 ring (mean Tl · · · F 3.095 Å); intermolecular Tl · · · S interactions between individual units of (**1**) give this material an extended-chain structure in the solid state. Crystalline (**2**) contains discrete molecular units of [(cp)Mo(μ-SC6F5)4Tl] in which Tl^I is co-ordinated by four S atoms (mean Tl–S 3.272 Å); these four S atoms, four closely associated *o*-F atoms, one from each C6F5 ring (mean Tl · · · F 3.062 Å), and the Mo atom [Mo · · · Tl 3.402(3) Å] define a cavity in which the Tl^I is situated. The anion [Mo(SC6F5)4(cp)]$^-$ in (**2**) is acting as a polydentate ligand to Tl$^+$. Variable-temperature ^{19}F n.m.r. studies on complexes (**1**) and (**2**) in toluene, dichloromethane, and acetone solutions establish the occurrence both of restricted rotation of the C6F5 groups and of solvent-dependent ionic dissociation into Tl$^+$ and [Mo(SC6F5)2L2(cp)]$^-$. Significant ionisation occurs in the polar solvent acetone, and this is supported by conductivity measurements. Reactions of complex (**1**) with tertiary phosphines give products [Mo(SC6F5)(CO)2L(cp)] [L = PMe2Ph (**3**), PMePh2 (**4**), or PPh3 (**5**)] with 'four-legged piano-stool' geometry; these complexes are principally *cis* isomers although minor amounts of *trans* isomers were detected by ^{1}H n.m.r. spectroscopy in solutions of (**3**) and (**5**). Reaction of complex (**2**) with PPh3 affords a species [TlMo(SC6F5)4(PPh3)2(cp)] which variable-temperature ^{1}H, ^{19}F, and ^{31}P n.m.r. studies show to exist as a mixture of two interchanging forms in solution.

Thiolates can act as terminal or bridging ligands in co-ordination compounds of most transition metals, in a range of oxidation states. Current interest in the varied structure and the chemical and redox reactivity of such compounds has been stimulated by the involvement of some systems in biological and catalytic processes.[1] In this context, molybdenum thiolates have received particular attention, and several monocyclopentadienyl thiolato complexes have been studied. Simple, mononuclear species, [Mo(SR)(CO)3(cp)] (R = alkyl or aryl; cp = η5-C5H5), can be synthesised but the tendency of thiolates to form μ bridges is exemplified by the facile dimerisation of these compounds to [Mo2(μ-SR)2(CO)4(cp)2];[2] the presence of more electron-withdrawing thiolate ligands (R = CF3 or C6F5) inhibits this dimerisation process.[2,3] Other mononuclear complexes include the co-ordinatively unsaturated derivatives [Mo(SC6F5)L(CF3C≡CCF3)(cp)] [L = CO, PR3, P(OMe)3, CF3C≡CCF3, or O],[4] [Mo(SPh)2(NO)(cp)],[5] and paramagnetic species [Mo(SR)2(η4-C4H6)(cp)] (R = C6H4Me-4 or C6F5).[6] Other reported binuclear complexes containing carbonyl ligands include unsaturated [Mo2(μ-SBu^t)2(CO)2-

(cp)2] (Mo=Mo)[7] and cationic [Mo2(μ-Bu^t)2(CO)4(cp)2]$^{2+}$ (Mo–Mo)[8] formed electrochemically from the neutral compound. Bridging thiolate ligands are present in a range of non-carbonyl binuclear derivatives, structurally related to the parent complex [Mo2(μ-SR)4(cp)2];[9] these show interesting ligand-based hydrogenation reactions.[10] Unsymmetrical species, *e.g.* [(cp)(OC)Mo(μ-SR)3Mo(CO)3],[11] and heteronuclear species, *e.g.* [(cp)(OC)$_n$Mo(μ-SR)W(CO)5] (n = 2 or 3)[12] are also known.
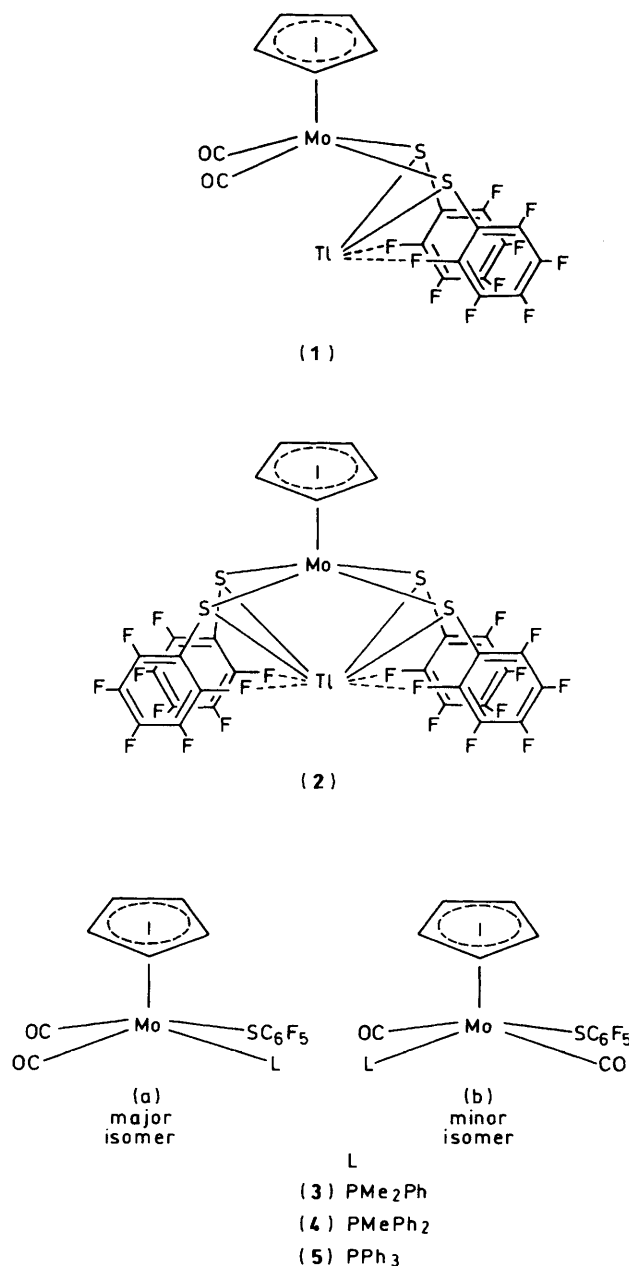
In this paper we report the characterisation of new anionic carbonyl and non-carbonyl complexes, [Mo(SC6F5)2L2(cp)]$^-$ (L = CO or SC6F5), their interaction with thallium(I) counter ions, and products of their reactions with some phosphines. Some aspects of this work have appeared in preliminary publications.[13]

Results and Discussion

Synthesis and General Characterisation of Complexes.—The reaction between Tl(SC6F5) and [MoCl(CO)3(cp)] (molar ratio 2:1) in diethyl ether at r.t. (room temperature) affords the red crystalline complex [TlMo(SC6F5)2(CO)2(cp)] (**1**) in good yield (78%). This reaction proceeds *via* the known derivative [Mo(SC6F5)(CO)3(cp)][3] and small amounts of the latter species are removed during the isolation of (**1**) by crystallisation. By using a molar ratio of 5:1 for Tl(SC6F5):[MoCl(CO)3(cp)]

(1)

(2)

(a)
major
isomer

(b)
minor
isomer

L

(3) PMe$_2$Ph

(4) PMePh$_2$

(5) PPh$_3$

Figure 1. Molecular structure of complex (1) (ORTEP[30])

and under the more forcing reaction conditions of a refluxing tetrahydrofuran medium, the red complex [TlMo(SC$_6$F$_5$)$_4$(cp)] (2) is produced in moderate yield (*ca.* 30%). Complex (2) can also be obtained by reaction of (1) with an excess of Tl(SC$_6$F$_5$) even at r.t., albeit in low yield. It may be noted that in the formation of complex (2) total replacement of carbonyl groups on the starting material by C$_6$F$_5$S$^-$ has occurred; also, the molybdenum has been oxidised from a formal oxidation state of +2 to +4. Presumably, this oxidation of the molybdenum has facilitated the replacement of the final two CO groups by the less effective π-acceptor ligands C$_6$F$_5$S$^-$ to give the formally 16-electron product (2). In fact, the electron-deficient complex (2) may be stabilised by electron π donation from the C$_6$F$_5$S$^-$ ligands. The oxidant in these reactions is Tl^I and, although not definitely identified, it may be assumed that thallium metal is the reduction product and this is removed from the reaction with the insoluble TlCl by-product and excess of Tl(SC$_6$F$_5$). It is pertinent that [W(SC$_6$F$_5$)(CO)$_3$(cp)] is the only product

obtained from reactions between [WCl(CO)$_3$(cp)] and Tl-(SC$_6$F$_5$), even in refluxing tetrahydrofuran, and no thallium derivatives of W^{II} or W^{IV} can be prepared by this route.[13a] This reflects the lower lability to substitution of carbonyl ligands on the tungsten relative to the molybdenum derivative.

Complex (2) can also be prepared in moderate yields from oxidative-substitution reactions by excess of Tl(SC$_6$F$_5$) on the molybdenum(II) complex [MoCl(CF$_3$C≡CCF$_3$)$_2$(cp)] or on the paramagnetic molybdenum(III) complexes [MoX$_2$(η^4-C$_4$H$_6$)-(cp)] (X = Cl or SC$_6$F$_5$). Reaction between [MoBr$_2$(CO)(η^3-C$_3$H$_5$)(cp)] and Tl(SC$_6$F$_5$) provides another route to complex (2) and in this case no change in the formal oxidation state of molybdenum occurs.

Electron impact (e.i.) mass spectra could not be obtained for complex (1) or (2) but field-desorption (f.d.) spectra of (2) exhibited a large peak of highest m/e value corresponding to the molecular formula [TlMo(SC$_6$F$_5$)$_4$(cp)]: the molecular weight of (2) in toluene (vapour-pressure osmometry) is also in accord with this non-dissociated (or non-associated) formula. However, in acetone solutions complex (1) and, more particularly, complex (2) shows significant electrical conductivity [(1), Λ_0 = 16; (2), Λ (10^{-3} mol dm^{-3}) = 78 Ω^{-1} cm^2 mol^{-1}]. This conductivity must be attributed to some dissociation into solvated ions Tl$^+$ and [Mo(SC$_6$F$_5$)$_2$L$_2$(cp)]$^-$ (X = CO or SC$_6$F$_5$) in the more polar solvent.[14]

Tertiary phosphines react with complex (1) in dichloromethane at r.t. to afford reasonable yields of red-pink complexes [Mo(SC$_6$F$_5$)(CO)$_2$L(cp)] [L = PMe$_2$Ph (3), PMePh$_2$ (4), or PPh$_3$ (5)]. These reactions involve displacement of Tl(SC$_6$F$_5$) from (1). Complexes (3)—(5) have been characterised by elemental analysis and by e.i. mass spectra which show molecular ions and prominent peaks attributable to [M − CO]$^+$, [M − 2CO]$^+$, and [M − (2CO + L)]$^+$. Complexes (3)—(5) each show two ν(CO) bands in the i.r. spectra (1 955—1 958, 1 874—1 878 cm^{-1}). These ν(CO) frequencies are almost identical to those of the parent complex (1) and this indicates that the phosphine ligand, L, has a similar electronic effect on two CO groups in (3)—(5) to that of Tl(SC$_6$F$_5$) in (1). The molecular formula and i.r. spectra support a *cis* square-based 'piano-stool' geometry for complexes (3)—(5). Such *cis* structures are in accord with n.m.r. studies (see below), although for (3) and (5) minor amounts of *trans* isomers are also detectable in solution, as found for some related complexes [MoX(CO)$_2$L(cp)].[15]

Complex (2) reacts with triphenylphosphine in dichloromethane at r.t. to form a red addition complex [TlMo-(SC$_6$F$_5$)$_4$(PPh$_3$)$_2$(cp)] (6). This formulation is supported by elemental analysis and by n.m.r. spectroscopy; the molecular structure has been investigated by the latter technique (see below). Reactions of complex (2) with other tertiary phosphines (PMe$_2$Ph, PMePh$_2$, and PEt$_3$) give intractable red products
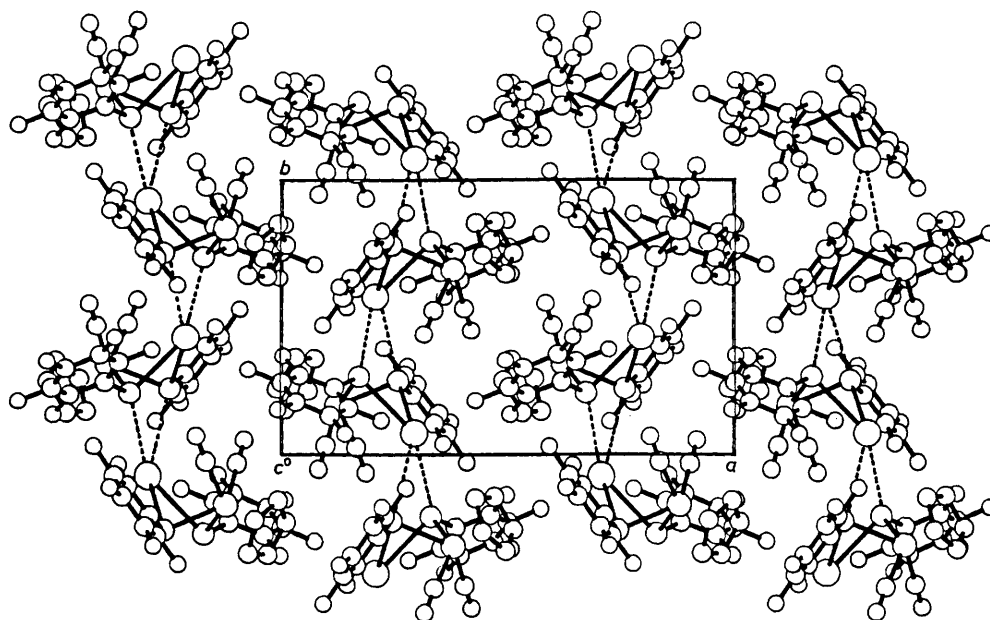
Figure 2. Crystal packing diagram for complex (**1**) as viewed along the c axis (PLUTO[31])

Table 1. Fractional co-ordinates of atoms with standard deviations for complex (**1**)

Atom	x	y	z
Tl	0.293 62(4)	0.075 21(7)	0.531 98(6)
Mo	0.121 80(7)	0.174 61(12)	0.352 58(11)
S(1)	0.257 62(22)	0.264 6(4)	0.346 3(3)
S(2)	0.171 23(22)	0.279 4(4)	0.539 1(3)
F(1)	0.225 0(6)	0.383 2(9)	0.118 2(9)
F(2)	0.277 6(7)	0.317 0(11)	−0.065 6(9)
F(3)	0.372 3(6)	0.111 3(10)	−0.065 2(8)
F(4)	0.408 9(6)	−0.029 5(9)	0.121 4(9)
F(5)	0.356 8(5)	0.036 5(9)	0.309 6(7)
F(6)	0.221 1(6)	0.121 1(11)	0.745 0(8)
F(7)	0.141 5(6)	0.074 7(11)	0.912 0(8)
F(8)	−0.006 3(6)	0.160 1(10)	0.902 8(7)
F(9)	−0.072 0(6)	0.305 6(11)	0.727 2(9)
F(10)	0.004 0(5)	0.356 4(10)	0.559 3(8)
C(1)	0.288 4(8)	0.211 2(14)	0.221 7(13)
C(2)	0.271 6(9)	0.283 7(15)	0.122 7(14)
C(3)	0.297 5(10)	0.249 4(18)	0.024 7(13)
C(4)	0.346 1(10)	0.142 4(17)	0.028 0(14)
C(5)	0.365 2(10)	0.072 1(16)	0.122 5(14)
C(6)	0.336 6(8)	0.108 2(16)	0.216 0(14)
C(7)	0.117 2(9)	0.239 4(13)	0.644 2(11)
C(8)	0.149 0(10)	0.165 3(17)	0.735 6(13)
C(9)	0.108 2(11)	0.138 8(16)	0.822 4(13)
C(10)	0.033 2(9)	0.188 1(15)	0.818 3(12)
C(11)	0.001 5(9)	0.258 7(15)	0.729 6(15)
C(12)	0.040 0(10)	0.284 2(15)	0.642 7(14)
C(13)	0.164 6(9)	0.024 6(17)	0.285 9(13)
O(1)	0.185 4(8)	−0.063 7(12)	0.250 2(11)
C(19)	0.097 5(9)	0.031 5(17)	0.445 8(16)
O(2)	0.081 9(7)	−0.050 1(12)	0.496 7(11)
C(14)	0.072 4(6)	0.346 1(11)	0.227 2(10)
C(15)	0.030 3(6)	0.350 7(11)	0.318 3(10)
C(16)	−0.010 6(6)	0.234 8(11)	0.320 9(10)
C(17)	0.006 1(6)	0.158 5(11)	0.231 5(10)
C(18)	0.057 4(6)	0.227 3(11)	0.173 6(10)

Table 2. Derived geometrical parameters (bond lengths in Å, angles in °) for complex (**1**) with standard deviations

Tl $\cdots$ Mo	3.518 0(10)	Mo–C(14)	2.427(11)
Tl–S(1)	2.998(4)	Mo–C(15)	2.431(11)
Tl–S(2)	3.032(4)	Mo–C(16)	2.335(11)
Tl $\cdots$ F(5)	3.099(9)	Mo–C(17)	2.268(11)
Tl $\cdots$ F(6)	3.090(10)	Mo–C(18)	2.327(11)
Mo–S(1)	2.538(4)	S(1)–C(1)	1.776(15)
Mo–S(2)	2.530(4)	S(2)–C(7)	1.752(15)
Mo–C(13)	1.981(16)	C(13)–O(1)	1.116(21)
Mo–C(19)	1.978(18)	C(19)–O(2)	1.121(22)
S(1)–Tl–S(2)	59.20(11)	Mo–C(13)–O(1)	176.1(15)
S(1)–Tl–Mo	44.97(8)	Mo–C(19)–O(2)	178.1(15)
S(2)–Tl–Mo	44.69(8)	C(13)–Mo–C(19)	75.3(7)
Mo–S(1)–Tl	78.41(11)	S(1)–Mo–C(13)	83.2(5)
Mo–S(2)–Tl	77.89(11)	S(1)–Mo–C(19)	126.2(5)
S(1)–Mo–S(2)	71.99(13)	S(2)–Mo–C(13)	128.6(5)
Mo–S(1)–C(1)	108.4(5)	S(2)–Mo–C(19)	84.2(5)
Mo–S(2)–C(7)	113.8(5)		

Solid-state Molecular Structure of [TlMo(SC$_6$F$_5$)$_2$(CO)$_2$-(cp)] (**1**).—A red prismatic crystal of (**1**), obtained from dichloromethane–hexane, was subjected to X-ray crystallographic analysis. Figure 1 presents a perspective view of a single molecule of this derivative and Figure 2 is a crystal-packing diagram indicating the nature of the intermolecular contacts between Tl and two sulphur atoms, S(1′) and S(2′), on a neighbouring symmetry-related ($\frac{1}{2} + x$, $-\frac{1}{2} + y$, $1 - z$) molecule. These interactions result in the formation of infinite chains which run roughly parallel to the b axis in the crystal (see Figure 2). Atomic fractional co-ordinates and important derived geometrical parameters are given in Tables 1 and 2, respectively. Each individual unit of complex (**1**) has approximately C_s symmetry about a plane including both Mo and Tl atoms and bisecting the angles C(13)–Mo–C(19) and S(1)–Mo–S(2).

The ligands adopt a 'piano-stool' co-ordination geometry about Mo with the two thiolate and two carbonyl ligands defining a square base. Geometrical parameters involving these ligands are as normally found. It should be noted that Mo–S

which could not be obtained analytically pure. These other products may be mixtures including complexes structurally related to (**6**).

Table 3. Fractional co-ordinates of atoms with standard deviations for complex (2)

Atom	x	y	z	Atom	x	y	z
Tl	0.106 15(6)	0.250 00	0.093 65(7)	C(3)	0.483 2(24)	0.314 6(17)	0.067 0(15)
Mo	0.337 62(14)	0.242 74(39)	0.047 77(13)	C(4)	0.485 2(11)	0.225 1(21)	0.096 6(13)
S(1)	0.253 7(5)	0.112 1(6)	−0.002 0(4)	C(5)	0.468 1(21)	0.169 4(11)	0.022 6(17)
S(2)	0.249 0(5)	0.312 5(6)	−0.071 9(4)	C(11)	0.220 8(8)	0.114 8(12)	−0.121 3(6)
S(3)	0.282 9(5)	0.377 7(6)	0.122 1(4)	C(12)	0.285 3(5)	0.092 0(11)	−0.185 5(9)
S(4)	0.295 9(5)	0.175 3(6)	0.192 0(4)	C(13)	0.262 6(8)	0.097 4(6)	−0.275 0(8)
F(12)	0.370 3(5)	0.064 6(15)	−0.160 9(13)	C(14)	0.175 4(7)	0.125 5(10)	−0.300 4(6)
F(13)	0.325 5(10)	0.075 2(6)	−0.337 6(11)	C(15)	0.110 8(6)	0.148 2(9)	−0.236 1(9)
F(14)	0.153 2(10)	0.130 7(15)	−0.387 5(7)	C(16)	0.133 5(8)	0.142 9(7)	−0.146 6(8)
F(15)	0.025 8(6)	0.175 6(13)	−0.260 8(12)	C(21)	0.215 5(7)	0.431 5(7)	−0.067 2(8)
F(16)	0.070 6(11)	0.165 1(8)	−0.084 1(11)	C(22)	0.277 5(5)	0.502 1(9)	−0.067 8(7)
F(22)	0.369 1(6)	0.485 7(11)	−0.066 9(11)	C(23)	0.245 5(6)	0.589 4(8)	−0.069 2(3)
F(23)	0.305 9(8)	0.658 1(10)	−0.069 8(4)	C(24)	0.151 5(7)	0.606 2(7)	−0.070 1(7)
F(24)	0.120 3(9)	0.691 3(8)	−0.071 5(11)	C(25)	0.089 4(5)	0.535 6(8)	−0.069 5(6)
F(25)	−0.002 2(5)	0.552 0(11)	−0.070 3(9)	C(26)	0.121 5(7)	0.448 3(8)	−0.068 0(5)
F(26)	0.061 1(9)	0.379 5(9)	−0.067 5(6)	C(31)	0.304 9(7)	0.385 2(11)	0.242 8(4)
F(32)	0.456 7(7)	0.435 0(7)	0.211 7(6)	C(32)	0.391 0(6)	0.413 3(7)	0.271 7(5)
F(33)	0.493 4(7)	0.446 7(13)	0.390 1(6)	C(33)	0.409 6(6)	0.419 3(9)	0.362 0(5)
F(34)	0.360 2(9)	0.402 8(14)	0.511 6(4)	C(34)	0.342 1(7)	0.397 0(9)	0.423 6(4)
F(35)	0.190 3(6)	0.347 2(6)	0.454 7(6)	C(35)	0.256 0(5)	0.368 8(6)	0.394 8(5)
F(36)	0.153 6(8)	0.335 4(14)	0.276 3(6)	C(36)	0.237 4(7)	0.362 9(10)	0.304 4(5)
F(42)	0.412 3(6)	0.009 8(10)	0.154 9(8)	C(41)	0.261 7(9)	0.056 9(7)	0.194 8(7)
F(43)	0.357 0(11)	−0.165 1(9)	0.160 1(13)	C(42)	0.324 2(6)	−0.010 7(8)	0.175 9(6)
F(44)	0.178 6(10)	−0.206 6(8)	0.202 6(9)	C(43)	0.296 2(8)	−0.099 3(8)	0.178 5(8)
F(45)	0.055 3(6)	−0.073 2(10)	0.240 0(9)	C(44)	0.205 8(8)	−0.120 3(7)	0.200 1(6)
F(46)	0.110 5(11)	0.101 7(8)	0.234 9(14)	C(45)	0.143 4(6)	−0.052 7(8)	0.219 0(7)
C(1)	0.455 5(20)	0.224 5(21)	−0.052 7(10)	C(46)	0.171 3(9)	0.035 9(7)	0.216 4(10)
C(2)	0.464 9(13)	0.314 2(17)	−0.025 2(17)				

distances in this formally molybdenum(II) complex are *ca.* 0.1 Å longer than in the molybdenum(IV) complex (2).

The Tl atom is located in a site distal to the cyclopentadienyl group and below the two carbonyl ligands and the molybdenum-co-ordinated S atoms of the thiolate ligands, being displaced from a central position towards these two S atoms. The Mo–Tl vector is at 10.3° to the vector from the Mo atom to the centroid of η^5-C_5H_5. The large separation between Mo and Tl atoms [3.518(1) Å] appears to preclude any significant direct metal–metal interaction. This $Tl^I \cdots Mo^{II}$ distance is *ca.* 0.1 Å longer than the $Tl^I \cdots Mo^{IV}$ distance in (2). The only previously reported Mo–Tl bonding distances are for $[Tl\{Mo(CO)_3(cp)\}_3]$ with an average separation between Tl^{III} and Mo^{II} of 2.965 Å;[16] a somewhat larger separation might be expected for $Tl^I \cdots Mo^{II}$.

The Tl–S distances, although on average *ca.* 0.25 Å shorter than in complex (2) (see below), are comparable to Tl–S bonds in compounds such as $[AuTl\{Ph_2P(CH_2)S\}_2]$,[17] though somewhat shorter than Tl–S contacts in $[\{Tl(S_2CNEt_2)\}_2]$,[18a] containing Tl^I co-ordinated by four S atoms (average Tl–S 3.07 Å), or in other more extended structures in which Tl^I–S interactions are observed (*e.g.* $Tl_2Mo_9S_{11}$,[18b] Tl_2SiS_4,[18c] Tl_3AsS_4,[18d] and other sulpho salts). Consequently there appears to be a significant bonding interaction between Tl^I and the two S atoms in complex (1), although this may be largely electrostatic in nature. The two intermolecular Tl $\cdots$ S contacts [3.333(3) and 3.772(3) Å] also contribute to the co-ordination sphere of Tl^I, creating a tetrasulphur ligand environment similar to that found for Tl^I in complex (2). The chain structure of solid (1) is of interest since the resulting one-dimensional heterobimetallic polymer, incorporating redox-active metal centres, has potential for novel physical properties. The recently reported luminescent properties of a one-dimensional polymer with Au–Tl bonds is of interest in this context.[17]

Both pentafluorophenyl groups are arranged such that one *ortho*-F atom on each ring approaches closely to Tl [Tl $\cdots$ F

3.099(9) and 3.090(10) Å]. These intramolecular Tl $\cdots$ F 'soft' contacts probably do not represent a significant bonding interaction between the atoms but may add to the stability of complexation of Tl^+ by $[Mo(SC_6F_5)_2(CO)_2(cp)]^-$ and may influence the conformation of the C_6F_5 rings. Similar interactions between *o*-F atoms in C_6F_5 groups and Ag have been reported in heterometallic platinum complexes.[19] In complex (1) the Mo atom, the two S atoms, and two *o*-F atoms on a single molybdenum entity combined with the two S atoms in the neighbouring entity partially encapsulate the Tl^I and this arrangement may be compared to the distinct cavity enclosing Tl^I in complex (2) (see below).

Solid-state Molecular Structure of $[TlMo(SC_6F_5)_4(cp)]$ (2).—A red-orange plate-like crystal of (2), obtained from ethyl acetate–diethyl ether solution, was subjected to X-ray crystallographic analysis. Figure 3 gives a perspective view of the structure of this complex which, unlike (1), exists as discrete molecular units in the solid state. Tables 3 and 4, respectively, list atomic fractional co-ordinates and selected, derived geometrical parameters. Assuming circular symmetry for the η-cyclopentadienyl group, individual molecules of (2) approach a point-group symmetry of C_4, with the Tl atom *trans* to the centroid of the η^5-C_5H_5 group across the central Mo atom and on the idealised axis of symmetry. The four S atoms lie below the Mo atom, on the same side as Tl, forming a square base for the 'piano-stool' geometry of the $MoS_4(\eta^5$-$C_5H_5)$ unit; a projection of the $Mo(SC_6F_5)_4$ fragment on to a plane perpendicular to the Mo–Tl axis has a 'swastika-like' arrangement. The plane of each C_6F_5 group is approximately parallel to the Mo–Tl axis and one *o*-F atom on each ring lies in close proximity to the Tl atom.

The Mo–S bonding distances (average 2.424 Å) are shorter than in complex (1), as might be expected for the higher formal oxidation state of Mo in (2). The Mo $\cdots$ Tl separation [3.402(3) Å], although also shorter than in complex (1), still appears to be

**Table 4.** Derived geometrical parameters (bond lengths in Å, angles in °) for complex (2)

Tl ⋯ Mo	3.402(3)	Tl–S(1)	3.276(9)
Tl–S(2)	3.342(7)	Tl–S(3)	3.200(8)
Tl–S(4)	3.292(8)	Tl ⋯ F(16)	2.978(1)
Tl ⋯ F(26)	3.144(1)	Tl ⋯ F(36)	3.080(1)
Tl ⋯ F(46)	3.046(1)	Mo–S(1)	2.402(8)
Mo–S(2)	2.425(8)	Mo–S(3)	2.420(9)
Mo–S(4)	2.447(8)	Mo–C(1)	2.278(3)
Mo–C(2)	2.379(4)	Mo–C(3)	2.368(4)
Mo–C(4)	2.259(3)	Mo–C(5)	2.201(4)
S(1)–C(11)	1.840(7)	S(2)–C(21)	1.832(9)
S(3)–C(31)	1.831(7)	S(4)–C(41)	1.825(10)
S(1)–Tl–S(2)	56.9(2)	S(1)–Tl–S(3)	85.0(2)
S(1)–Tl–S(4)	56.4(2)	S(2)–Tl–S(3)	56.3(2)
S(2)–Tl–S(4)	85.0(2)	S(3)–Tl–S(4)	58.7(3)
S(1)–Mo–S(2)	81.6(3)	S(1)–Mo–S(3)	130.2(3)
S(1)–Mo–S(4)	79.5(3)	S(2)–Mo–S(3)	79.2(3)
S(2)–Mo–S(4)	133.8(3)	S(3)–Mo–S(4)	81.8(3)
Tl–S(1)–Mo	71.7(3)	Tl–S(1)–C(11)	103.9(4)
Mo–S(1)–C(11)	114.2(4)	Tl–S(2)–Mo	70.2(2)
Tl–S(2)–C(21)	94.4(3)	Mo–S(2)–C(21)	121.5(4)
Tl–S(3)–Mo	73.0(3)	Tl–S(3)–C(31)	107.7(4)
Mo–S(3)–C(31)	116.3(4)	Tl–S(4)–Mo	71.0(2)
Tl–S(4)–C(41)	96.4(3)	Mo–S(4)–C(41)	118.7(4)
S(1)–C(11)–C(12)	119.5(3)	S(1)–C(11)–C(16)	120.4(3)
S(2)–C(21)–C(22)	124.2(3)	S(2)–C(21)–C(26)	115.7(3)
S(3)–C(31)–C(32)	118.7(3)	S(3)–C(31)–C(36)	121.3(3)
S(4)–C(41)–C(42)	121.4(3)	S(4)–C(41)–C(46)	118.6(3)

Figure 3. Molecular structure of complex (2) (ORTEP[30])

too long to permit substantial direct metal–metal interaction. The Tl atom is co-ordinated by the four S atoms (mean Tl–S 3.272 Å) and although these Tl–S separations are 0.2—0.3 Å greater than in complex (1), they are comparable to bonding distances in other Tl^I–S complexes.[17,18] This lengthening of Tl–S bonds in (2) relative to (1) probably reflects the severe intramolecular steric congestion within the former complex and the mainly electrostatic nature of these Tl^I–S interactions. No short intermolecular Tl ⋯ S contracts are observed for complex (2). The 'soft' contacts between four o-F atoms and Tl (average 3.062 Å) are comparable to those observed between the two C_6F_5 rings and Tl in complex (1) and may contribute to the stability and conformation of the complexation of Tl^+ by $[Mo(SC_6F_5)_4(cp)]^-$.

From the crystal structure of (2) it is interesting that Tl^I is situated in a cavity of the $Mo(SC_6F_5)_4(cp)$ unit, bounded by the Mo atom, four S atoms, and four o-F atoms. Thus, the complex anion $[Mo(SC_6F_5)_4(cp)]^-$ is acting as a polydentate ligand, partially encapsulating the Tl^+ cation. This sequestration of a metal ion by an organometallic anion may have potential applications in areas such as metal-ion separation and metal-ion sensors, a possibility we are at present investigating.

N.M.R. Studies in Solution.—Selected ^{19}F n.m.r. data for complexes (1)—(6) are listed in Table 5 and other n.m.r. parameters are given in the Experimental section. In solution it appears that complex (1), as well as (2), is unassociated and both species show only one singlet resonance assignable to η^5-C_5H_5 in the ^1H n.m.r. spectra at ambient or low temperatures.

The ^{19}F n.m.r. spectrum of complex (1) at $-100\,°C$ in $[^2H_8]$toluene–diethyl ether (1:1) is in accord with the solid-state structure but without intermolecular Tl ⋯ S interactions; *i.e.* one o-F atom on each ring is closely associated with $^{205/203}Tl$ ($I = \frac{1}{2}$) giving rise to a resonance with a large doublet coupling ($\delta = -130.2$ p.p.m., $J = 3\,770$ Hz) whereas the other two o-F atoms give a single resonance ($\delta = -130.6$ p.p.m.) with a small poorly resolved doublet splitting ($J \approx 70$ Hz)
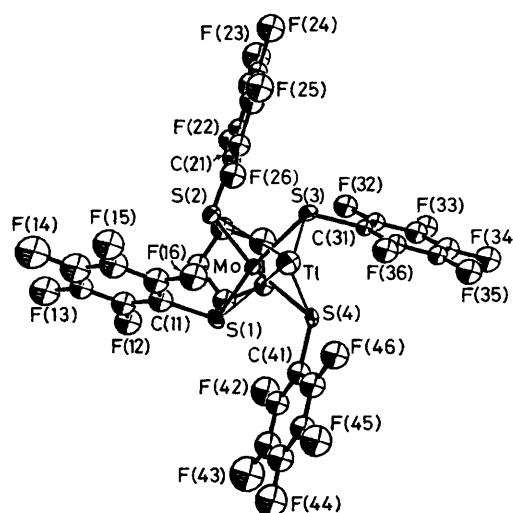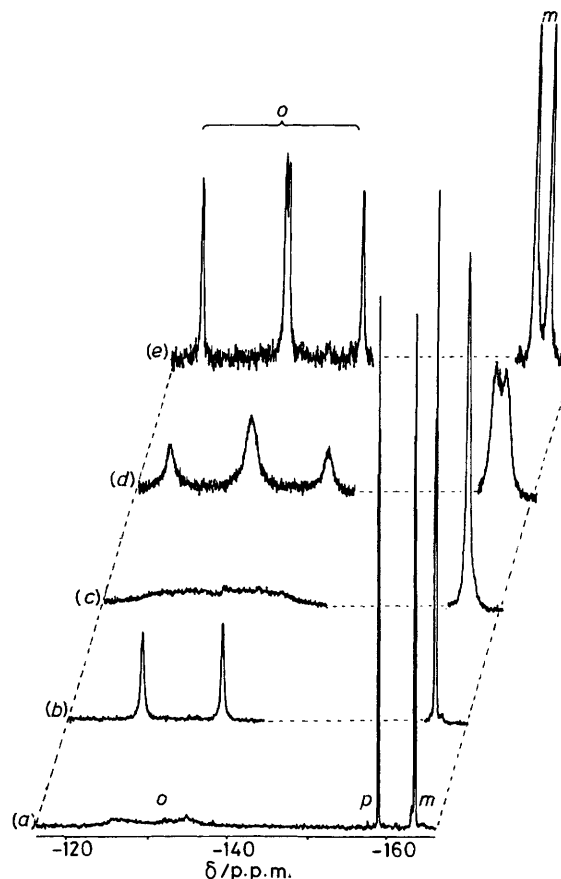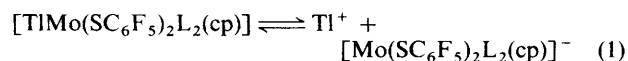

Figure 4. ^{19}F N.m.r. spectra of complex (1) in $C_6D_5CD_3$ at (a) $+20$, (b) -50, (c) -79, (d) -91, and (e) $-100\,°C$ $[C_6D_5CD_3$–Et_2O (1:1)]. The resonance of the p-F atoms (p) has been omitted from spectra (b)—(e)

probably arising from a long-range interaction with $^{205/203}Tl$ *via* a 'W-type' bond arrangement. It may be noted that, as in previous reports,[20] no distinction between coupling to ^{205}Tl and ^{203}Tl can be made. The rigid conformation of the two C_6F_5 rings is also supported by the two resonances for *meta*-F atoms assignable to the two inequivalent sites on each ring and by the single resonance for the equivalent *para*-F atoms (see Figure 4).

Table 5. ^{19}F N.m.r. parameters (δ in p.p.m., J in Hz) for complexes (1)—(6)

Complex	Solvent	Temperature/°C	
(1)	$C_6D_5CD_3$–Et_2O (1:1)	−100	−130.2 [d, J(Tl–F) 3 770, 2 o-F], −130.6 [d, J(Tl–F) 70, 2 o-F], −158.7 (br s, 2 p-F), −161.9 (br s, 2 m-F), −163.7 (br s, 2 m-F)
	$C_6D_5CD_3$	−50	−130.4 [d, J(Tl–F) 1 905, 4 o-F], −157.3 [t, J (F–F) 20, 2 p-F], −162.4 (m, 4 m-F)
	CD_2Cl_2	−60	−130.6 [d, J(Tl–F) 1 809, 4 o-F], −157.2 [t, J(F–F) 21.7, 2 p-F], −162.3 (m, 4 m-F)
	CD_2Cl_2	+20	−130.0 (vbr s, 4 o-F), −157.4 [t, J(F–F) 21, 2 p-F], −162.5 (m, 4 m-F)
	$(CD_3)_2CO$	−96	−130.4 [br d, J (Tl–F) $\approx$ 1 500, 4 o-F], −159.5 [t, J(F–F) 21.6, 2 p-F], −163.0 (br s, 4 m-F)
	$(CD_3)_2CO$	+3	−129.8 [d, J(F–F) 24, 4 o-F], −159.6 [t, J(F–F) 21, 2 p-F], −163.5 (m, 4 m-F)
(2)	$C_6D_5CD_3$	−79	−128.7 [d, J(Tl–F) 3 630, 4 o-F], −131.3 (m, 4 o-F), −154.1 [t, J(F–F) 22, 4 p-F], −160.5 (m, 4 m-F), −162.8 (m, 4 m-F)
	$C_6D_5CD_3$	+18	−129.8 [d, J(Tl–F) 1 770, 8 o-F], −155.2 [t, J (F–F) 21.3, 4 p-F], −162.4 (m, 8 m-F)
	$C_6D_5CD_3$	+92	−129.5 [br d, J(Tl–F) 1 750, 8 o-F], −155.5 [t, J(F–F) 20.6, 4 p-F], −162.7 (m, 8 m-F)
	CD_2Cl_2	−99	−128.3 [br d, J(Tl–F) 3 440, 4 o-F], −130.7 (br s, 4 o-F), −154.1 [t, J(F–F) 22, 4 p-F], −160.4 (m, 4 m-F), −162.5 (br s, 4 m-F)
	CD_2Cl_2	+20	−129.9 [br d, J(Tl–F) $\approx$ 1 700, 8 o-F], −155.5 [t, J(F–F) 21, 4 p-F], −162.6 (m, 8 m-F)
	$(CD_3)_2CO$	−93	$ca.$ −128.5 (vbr s, 4 o-F), −132.0 (s, 4 o-F), −157.9 (s, 4 p-F), −163.3 (s, 4 m-F), −164.6 (s, 4 m-F)
	$(CD_3)_2CO$	+20	−130.1 [d, J(F–F) 20.5, 8 o-F], −159.6 [t, J(F–F) 20.6, 4 p-F], −165.4 (m, 8 m-F)
(3)	$CDCl_3$	+20	−132.9 (m, 2 o-F), −159.6 [t, J(F–F) 21, 1 p-F], −164.3 (m, 2 m-F)
(4)	$CDCl_3$	+20	−132.3 (m, 2 o-F), −159.4 [t, J(F–F) 21, 1 p-F], −164.1 (m, 2 m-F)
(5)	$CDCl_3$	+20	−131.9 (m, 2 o-F), −159.5 [t, J(F–F) 21, 1 p-F], −164.3 (m, 2 m-F)
(6)	$C_6D_5CD_3$	−70	(a) (rel. int. 1): −128.5 [d, J(Tl–F) 3 613, 4 o-F], −131.1 (br s, 4 o-F), −154.3 (t, 4 p-F), −160.6 (m, 4 m-F), −162.9 (m, 4 m-F) (b) (rel. int. 3): −129.9 (br s, 4 o-F), −131.5 (br s, 4 o-F), −157.9 (br s, 4 p-F), −162.4 (br s, 4 m-F), −164.9 (br s, 4 m-F)
	CD_2Cl_2	−90	(a) (rel. int. 1): −128.3 [d, J(Tl–F) 3 412, 4 o-F], −130.9 (br s, 4 o-F), −154.5 (br s, 4 p-F), −160.8 (br s, 4 m-F), $ca.$ −163 [obscured by (b), 4 m-F] (b) (rel. int. 3): −129.3 (br s, 4 o-F), −132.7 (br s, 4 o-F), −157.2 (br s, 4 p-F), −162.9 (br s, 4 m-F), −164.5 (br s, 4 m-F)
	CD_2Cl_2	+30	−130.7 (br s, 8 o-F), −158.2 [t, J(F–F) 21, 4 p-F], −164.5 (m, 8 m-F)

In pure toluene a related spectrum is observed at −91 °C but at this higher temperature all peaks are somewhat broadened; at −88 °C the two m-F resonances coalesce and at $ca.$ −80 °C the *ortho* resonances also coalesce, forming a doublet at higher temperatures which is relatively sharp at −50 °C ($J = 1$ 905 Hz). The latter doublet represents an average J(Tl–F) coupling to all four o-F atoms and arises from rotation of the C_6F_5 rings about the SC_6F_5 bond which is rapid on the n.m.r. time-scale at this temperature. From coalescence of the m-F resonances it may be calculated[21] that $\Delta G_c^{\ddagger}$ (−88 °C) = 34.4 ± 0.5 kJ mol^{-1} for this rotation. Above −25 °C the doublet components of the o-F resonance broaden in a secondary process which may be attributed to kinetically significant ionic dissociation at these temperatures [equation (1), L = CO]. This dissociation is

$$[\text{TlMo}(\text{SC}_6\text{F}_5)_2\text{L}_2(\text{cp})] \rightleftharpoons \text{Tl}^+ + \\ [\text{Mo}(\text{SC}_6\text{F}_5)_2\text{L}_2(\text{cp})]^- \quad (1)$$

supported by studies in more polar solvents but does not occur to such an extent in toluene as to cause loss of coupling J(Tl-o-F) at 20 °C.

In polar solvents ionic dissociation of complex (1) occurs more easily and this is supported by conductivity measurements. Thus, the ^{19}F n.m.r. spectrum in dichloromethane at −89 °C is comparable to that observed in toluene at $ca.$ −75 °C and in the former solvent between −75 and −60 °C the spectrum is consistent with a non-dissociated entity [TlMo(SC_6F_5)$_2$(CO)$_2$(cp)] undergoing rapid C_6F_5 ring rotation and showing a sharp doublet [J(Tl–F) = 1 810 Hz] for all o-F atoms; at higher temperatures this doublet broadens and coalesces ($ca.$ −1 °C) to give a broadened singlet at 20 °C as ionic dissociation removes Tl–F coupling. In the more polar solvent $(CD_3)_2CO$, even at −96 °C, the o-F atoms give rise to a

broadened doublet due to significant ionic dissociation, equation (1), and at 3 °C a sharp single o-F resonance [with small, well resolved J(F–F) couplings] is observed. Thus, in acetone at ambient temperature rapid ionic dissociation is occurring.

Variable-temperature ^{19}F n.m.r. spectra of complex (2) bear some resemblance to those of complex (1), see Figures 5—7. In toluene at $\leqslant$ −80 °C the spectrum corresponds to the rigid, solid-state structure with two sets of four equivalent o-F and m-F resonances and one p-F resonance: all resonances show resolved J(F–F) couplings but only the four o-F atoms interacting with Tl show a large doublet coupling [J(Tl–F) = 3 630 Hz]. Rotation of the C_6F_5 rings becomes kinetically significant at higher temperatures and coalescence of m-F resonances occurs at $ca.$ −38 ± 5 °C, giving $\Delta G_c^{\ddagger}$ = 43.6 ± 1.0 kJ mol^{-1}; o-F resonances merge around −20 °C and at ambient temperature give rise to a doublet with broadened components [J(Tl–F) = 1 760 Hz] due to rapid rotation and average coupling to Tl, observed at both 188.31 and 75.40 MHz. The higher barrier to C_6F_5 rotation in complex (2) compared to that in (1) is probably associated with the greater steric hindrance of the four C_6F_5 rings in (2). As found for complex (1), there is no evidence for ionic dissociation of Tl$^+$ from (2) in toluene [equation (1), L = SC_6F_5] at or below room temperature, but the onset of significant dissociation is probably indicated by extensive broadening of the o-F doublet by +91 °C.

In dichloromethane, ionic dissociation influences the ^{19}F n.m.r. spectrum even at −98 °C when C_6F_5 rotation is still slow on the n.m.r. time-scale (Figure 6); thus, only a very broadened doublet is observed for the inner o-F atoms whereas the outer o-F atoms and the two sets of m-F atoms give sharper individual resonances. Coalescence of m-F atoms in CH_2Cl_2 ($ca.$ −30 °C) gives $\Delta G_c^{\ddagger}$ = 45.8 ± 1.0 kJ mol^{-1}. The o-F resonances merge
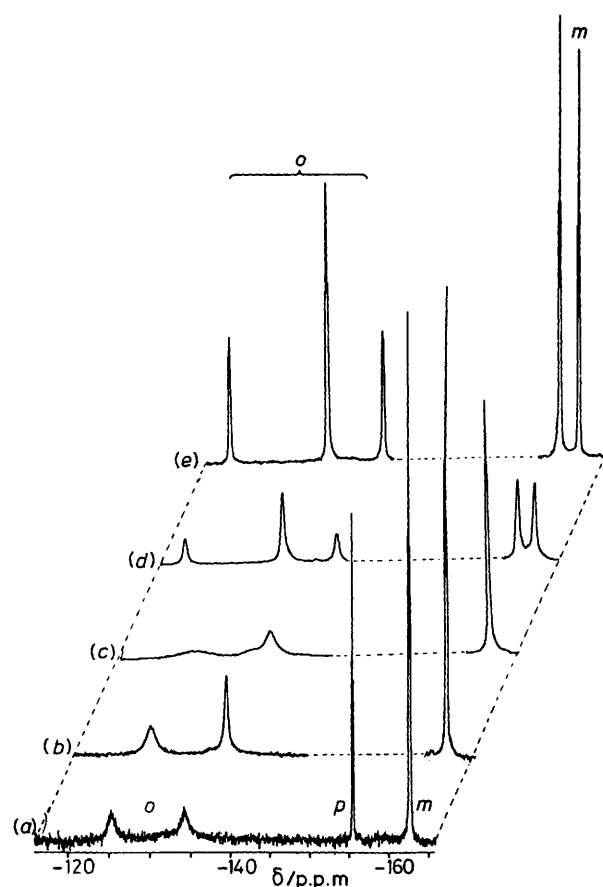
Figure 5. ^{19}F N.m.r. spectra of complex (2) in $C_6D_5CD_3$ at (a) +92, (b) +18, (c) −2, (d) −48, and (e) −79 °C. The resonance of the p-F atoms (p) has been omitted from spectra (b)—(e)

Figure 6. ^{19}F N.m.r. spectra of complex (2) in CD_2Cl_2 at (a) +20, (b) −19, (c) −39, (d) −58, and (e) −99 °C. The resonance of the p-F atoms (p) has been omitted from spectra (b)—(e)

around −20 °C, giving a doublet with broadened components [J(Tl–F) ≈ 1 700 Hz] at room temperature. In acetone, dissociation of Tl$^+$, equation (1), is of sufficient importance to affect all ^{19}F n.m.r. spectra from −93 °C (Figure 7); at −93 °C C_6F_5 rotation has been frozen out but this is rapid at higher temperatures with m-F coalescence at −70 °C, giving $\Delta G_c^{\ddagger}$ = 38.8 ± 0.7 kJ mol^{-1}. It may be noted that comparable values of $\Delta G^{\ddagger}$ for C_6F_5 rotation are calculated for solutions of complex (2) in toluene or dichloromethane whereas in acetone the lower value of $\Delta G^{\ddagger}$ must reflect the greater degree of ionic dissociation of Tl$^+$. At temperatures above −15 °C in acetone the spectrum of (2) exhibits three well resolved ^{19}F resonances typical of four equivalent, symmetrical C_6F_5 groups with expected F–F couplings but without any Tl–F coupling. The apparently more facile ionic dissociation of complex (2) compared to (1) is consistent with the higher electrical conductivity of (2) in acetone solution.

In conclusion, the ^{19}F n.m.r. data indicate that both complexes (1) and (2) exhibit two types of dynamic behaviour in solution. The first involves restricted rotation of the C_6F_5 groups about the C–S bond whereas the second may be attributed to ionic dissociation according to equation (1). The latter process is solvent dependent and the extent to which it occurs increases in the order toluene < dichloromethane < acetone, reflecting increasing solvent polarity.

Complexes (1) and (2) were investigated by ^{205}Tl n.m.r. spectroscopy but only at ambient temperature and in polar solvents in which solutions of suitable concentration could be obtained. Complex (1) in acetone or dichloromethane shows a
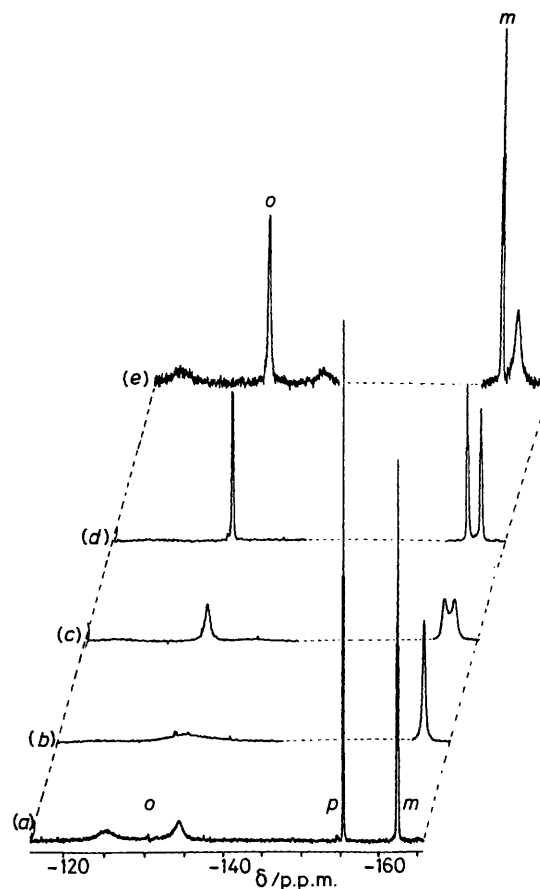
single broad ^{205}Tl resonance with a markedly solvent-dependent chemical shift; no resonances could be detected for complex (2) and extensive broadening may be occurring for this species. The broadening may be attributed to ionic dissociation and may be compounded by multiple o-F–Tl coupling.

Complexes (3)—(5) each show a singlet resonance in the ^{1}H n.m.r. spectrum, assignable to η^5-C_5H_5 of the cis isomer (a); appropriate resonances for the phosphine ligands include two signals for the diastereotopic methyl groups of PMe$_2$Ph in complex (3). cis Isomers of complexes (3) and (5) are in equilibrium with small amounts of the trans isomer (b) in solution [ratio cis: trans; (3), 31:1; (5), 17:1]. The trans isomers exhibit a doublet ^{1}H resonance for the η^5-C_5H_5 group with J(P–H) ≈ 2 Hz and a single resonance for equivalent methyl groups of PMe$_2$Ph in (3) which contains a plane of symmetry.[15] The ^{19}F n.m.r. spectra of complexes (3)—(5) show resonances typical of a C_6F_5 group undergoing unrestricted rotation at ambient temperature.

Low-temperature ^{1}H, ^{19}F, and ^{31}P-{^{1}H} n.m.r. spectra of complex (6) show that two forms, (6a) and (6b), are in equilibrium in toluene or dichloromethane solutions with relative concentrations ca. 1:3, respectively (Table 5). At ambient temperatures these two species are undergoing rapid interchange on the n.m.r. time-scale so that only one set of well resolved time-averaged ^{1}H or ^{19}F n.m.r. signals is observed, consistent with the presence of one η^5-C_5H_5 group or equivalent, symmetric C_6F_5 groups, respectively. Representative ^{19}F n.m.r. spectra are given in Figure 8.
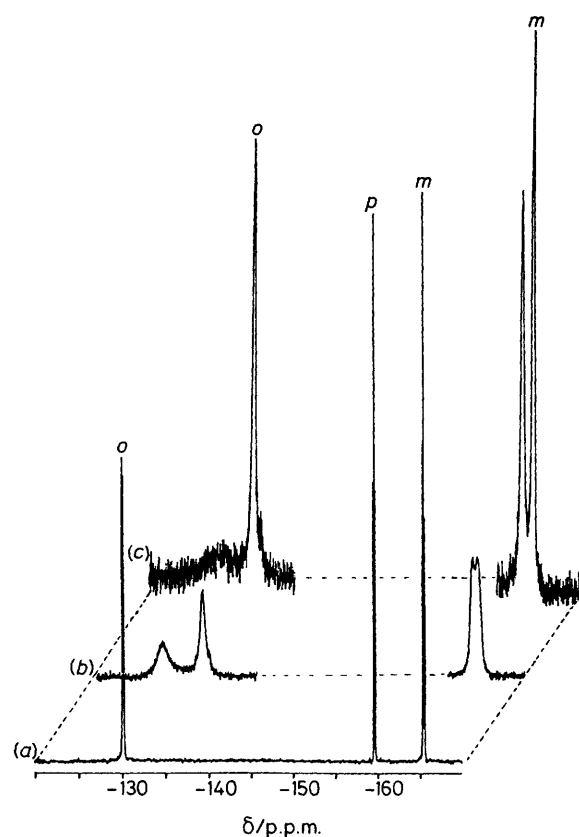
At low temperature the ^{1}H n.m.r. spectrum of the minor

Figure 7. ^{19}F N.m.r. spectra of complex (**2**) in $(CD_3)_2CO$ at (*a*) $+20$, (*b*) -72, and (*c*) $-93\,^{\circ}C$. The resonance of the *p*-F atoms (*p*) has been omitted from spectra (*b*) and (*c*)

Figure 8. ^{19}F N.m.r. spectra of complex (**6**): (*a*) in CD_2Cl_2 at $+30\,^{\circ}C$, (*b*) in CD_2Cl_2 at $-90\,^{\circ}C$, and (*c*) in $C_6D_5CD_3$ at $-70\,^{\circ}C$. Resonances assigned to isomer (**6a**) are marked with an asterisk

isomer, (**6a**), comprises a doublet η^5-C_5H_5 ($J \approx 5$ Hz) and multiplet PPh_3 resonances, the ^{31}P-$\{^1H\}$ spectrum shows a broadened singlet ($\delta \approx 36$ p.p.m.), and the ^{19}F n.m.r. is similar to that of complex (**2**) showing rigid C_6F_5 groups with two *o*- and two *m*-F resonances and one *o*-F resonance exhibiting a large Tl–F coupling ($J \approx 3\,500$ Hz). No P–F coupling can be assigned, in addition to which no change was observed in the cyclopentadienyl group ^1H doublet on irradiation of phosphorus, indicating that the splitting arises from coupling to thallium. A structure for isomer (**6a**), consistent with the n.m.r. data, is shown in Figure 9. The low-temperature ^{19}F n.m.r. spectrum indicates that the Tl^I must be co-ordinated to the S atoms in a similar manner to Tl^I in complex (**2**) but the presence of two PPh_3 groups modifies the system to the extent that spin–spin coupling now occurs between Tl and the H atoms of the distal C_5H_5 group. The PPh_3 groups are probably co-ordinated to Tl^I but the absence of Tl–P coupling in the ^{31}P n.m.r. spectrum suggests a rapid interchange between co-ordinated and free PPh_3 in solution, as illustrated in Figure 9.

The major component, (**6b**), at low temperature exhibits a singlet η^5-C_5H_5 resonance in its ^1H n.m.r. spectrum, a singlet ^{31}P-$\{^1H\}$ resonance, and a ^{19}F n.m.r. spectrum of five, somewhat broadened, singlet resonances assignable to the *p*-F, two inequivalent *m*-F, and two inequivalent *o*-F atoms of equivalent C_6F_5 groups held rigidly in an unsymmetric environment. No large Tl–F coupling occurs and, moreover, no other significant resolvable coupling between P, F, Tl, or H atoms is observable. These n.m.r. data suggest that isomer (**6b**) has a structure in which Tl^I is not closely associated with the anion [$Mo(SC_6F_5)_4(cp)$]$^-$ and in solution an ion pair is a probable structure, as in Figure 9. This ion pair is related to the

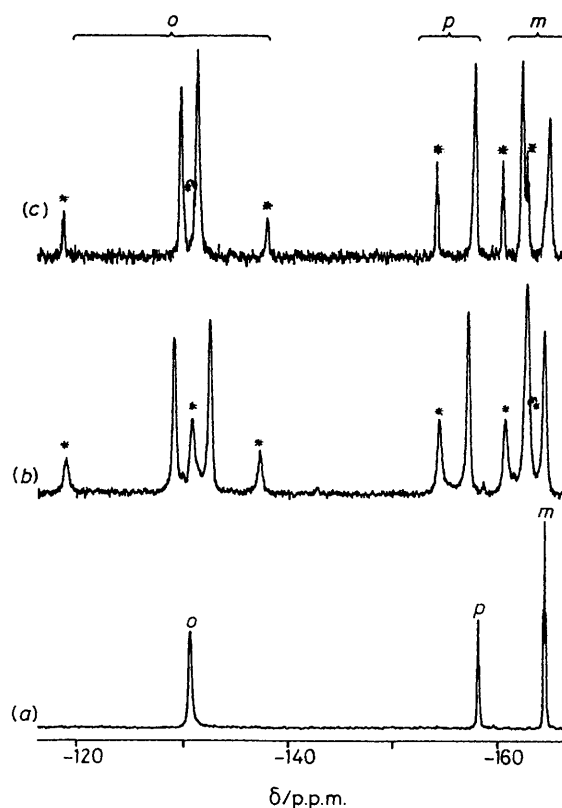structure of the salt [$N(PPh_3)_2$]$^+$[$Mo(SC_6F_5)_4(cp)$]$^-$.[13a,22] As for isomer (**6a**), the lack of Tl–P coupling in the ^{31}P n.m.r. spectrum of (**6b**) must be attributed to facile dissociation of the cation [$Tl(PPh_3)_2$]$^+$ in an equilibrium with unco-ordinated PPh_3.

Experimental

All reactions and operations were conducted under an atmosphere of dry, oxygen-free nitrogen gas, using Schlenk-type techniques and with solvents purified as described previously.[4,6] The starting materials [$MoCl(CO)_3(cp)$],[23] [$MoBr_2(CO)(\eta^3$-$C_3H_5)(cp)$],[24] [$MoCl(CF_3C{\equiv}CCF_3)_2(cp)$],[25] and [$MoCl_2(\eta^4$-$C_4H_6)(cp)$][6] were prepared by literature methods and the phosphines, obtained commercially (Strem or Aldrich), were used as supplied. The salt $Tl(SC_6F_5)$ was prepared from $Tl(O_2CMe)$ and C_6F_5SH (Aldrich) in methanol.

N.m.r. spectra, ^1H, ^{19}F, ^{31}P, and ^{13}C, were recorded at variable temperatures on a Bruker WP 200 SY spectrometer at 200.13, 188.31, 81.02, and 50.32 MHz, respectively, using SiMe$_4$, CCl$_3$F, 85% H_3PO_4, and SiMe$_4$ ($\delta = 0$ p.p.m.) as references. The ^{19}F n.m.r. spectra of complex (**2**) were also recorded on a Bruker WP 80 SY instrument at 75.40 MHz to confirm J(Tl–F) values; ^{205}Tl n.m.r. (51.7 MHz) spectra with shifts relative to $\Xi_{ref} = 57.683\,833$ MHz were obtained on a JEOL FX90 instrument at the City of London Polytechnic. I.r. spectra were measured in solution ($CHCl_3$) on a Perkin-Elmer 580 spectrometer and e.i. mass spectra on a Vacuum Generator's updated AEI MS9 at 70 eV (*ca.* 1.12×10^{-17} J). Field desorption (f.d.) mass spectra (4 and 6 kV) were run at the University of Tübingen, West Germany. Conductivity measure-
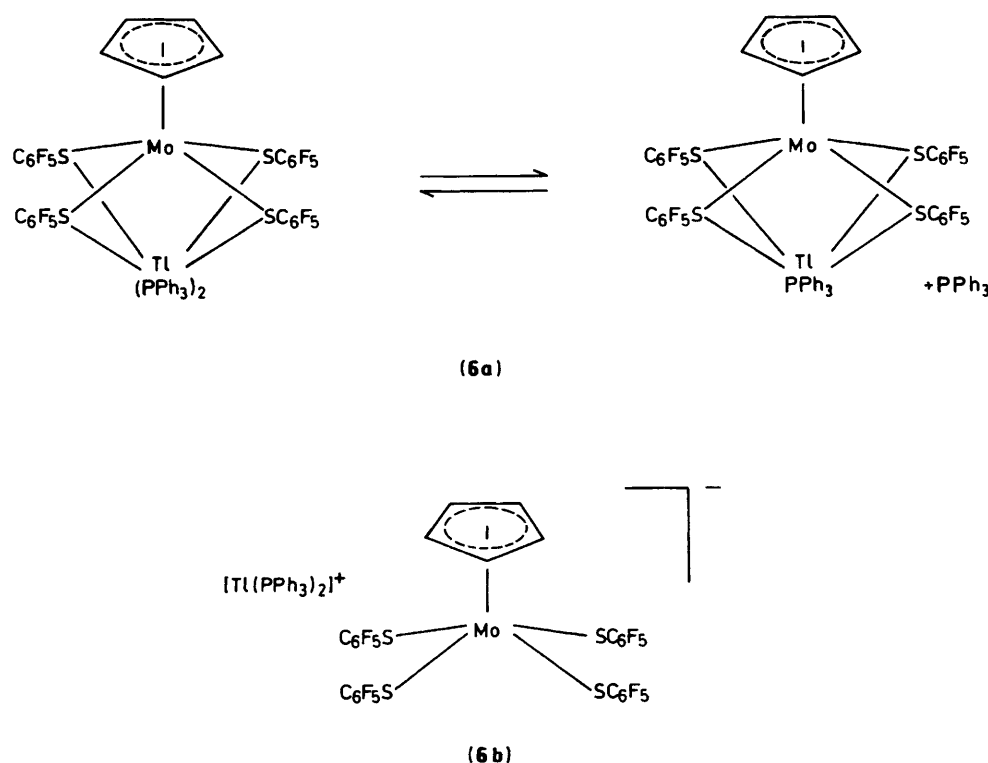
(6a)

(6b)

Figure 9. Structures for isomeric forms of complex (**6**) consistent with spectroscopic data

ments were made on 10^{-2}—10^{-4} mol dm^{-3} solutions in acetone at 25 °C, using a Wain Kerr Multi Bridge 6425.

Elemental analyses and the molecular-weight determination of complex (**2**) were carried out at Analytical Laboratories, Engelskirchen, West Germany and at the University of Manchester Institute of Science and Technology.

Preparation of [TlMo(SC$_6$F$_5$)$_2$(CO)$_2$(cp)] (**1**).—The compound [MoCl(CO)$_3$(cp)] (1 g, 3.57 mmol) and Tl(SC$_6$F$_5$) (2.88 g, 7.14 mmol) were stirred in diethyl ether (40 cm^3) at room temperature for 46 h giving a cloudy red solution. The reaction mixture was filtered and reduced in volume (*in vacuo*); hexane (10 cm^3) was added and the solution cooled to -15 °C to give red crystals of (**1**) (2.25 g, 78%) (Found: C, 28.4; H, 0.7; S, 8.3. Calc. for C$_{19}$H$_5$F$_{10}$MoO$_2$S$_2$Tl: C, 27.8; H, 0.6; S, 7.8%). I.r. (CHCl$_3$): ν(CO) 1 955 and 1 875 cm^{-1}. Λ_0 16 Ω^{-1} cm^2 mol^{-1} (by extrapolation of Λ values from 10^{-2}—10^{-4} mol dm^{-3} solutions). N.m.r.: ^{1}H (C$_6$D$_5$CD$_3$, 20 °C), δ 5.06 (s, C$_5$H$_5$); ^{205}Tl (CH$_2$Cl$_2$, r.t.), δ 1 225 (ν$_{\frac{1}{2}}$ 1 000); [(CD$_3$)$_2$CO, r.t.] 828 p.p.m. (ν$_{\frac{1}{2}}$ 600 Hz).

Preparation of [TlMo(SC$_6$F$_5$)$_4$(cp)] (**2**).—This complex was prepared by several different routes.

(*a*) The compound [MoCl(CO)$_3$(cp)] (0.16 g, 0.57 mmol) and Tl(SC$_6$F$_5$) (1.2 g, 2.78 mmol) were refluxed in tetrahydrofuran (40 cm^3) for 5 d to give a dark red solution. The solvent was completely removed *in vacuo* and the residue extracted with dichloromethane. The red solution was filtered, reduced in volume, mixed with hexane, and cooled at -15 °C to afford red microcrystalline (**2**) (0.19 g, 29%).

(*b*) The compound [MoCl(CF$_3$C$_2$CF$_3$)$_2$(cp)] (0.20 g, 0.38 mmol) and Tl(SC$_6$F$_5$) (0.620 g, 1.54 mmol) were stirred at r.t. in tetrahydrofuran (40 cm^3) for 12.5 h to form a red solution. The volatiles were removed *in vacuo*, the product extracted with dichloromethane, and purified as above. Yield of (**2**): 0.13 g (29%).

(*c*) The compound [TlMo(SC$_6$F$_5$)$_2$(CO)$_2$(cp)] (0.80 g, 0.98

mmol) and Tl(SC$_6$F$_5$) (1.50 g, 3.7 mmol) were stirred in dichloromethane (30 cm^3) at r.t. for 6 d. The solution was filtered, reduced in volume, and mixed with hexane. Cooling at -15 °C afforded (**2**) (0.11 g, 10%).

(*d*) The compound [MoBr$_2$(CO)(η^3-C$_3$H$_5$)(cp)] (0.20 g, 0.51 mmol) and Tl(SC$_6$F$_5$) (1.03 g, 2.55 mmol) were stirred in dichloromethane at r.t. for 24 h. The red solution was filtered and reduced in volume. Addition of hexane and cooling to -15 °C afforded (**2**) (0.11 g, 10%).

(*e*) [MoCl$_2$(η^4-C$_4$H$_6$)(cp)] (0.35 g, 1.2 mmol) and Tl(SC$_6$F$_5$) (2.0 g, 5.0 mmol) were stirred in tetrahydrofuran (50 cm^3) for 36 h at r.t. The red solution was filtered and evaporated to dryness. Extraction of the residue with dichloromethane, filtration, and evaporation of this solution yielded (**2**) contaminated with a little purple [Mo(SC$_6$F$_5$)$_2$(η^4-C$_4$H$_6$)(cp)]. Recrystallisation from toluene gave pure red microcrystalline (**2**), *ca.* 30% (Found: C, 30.4; H, 0.8; S, 11.1; Tl, 17.5. Calc. for C$_{29}$H$_5$F$_{20}$MoS$_4$Tl: C, 30.0; H, 0.45; S, 11.0; Tl, 17.6%); *M* (toluene) 1 100; calc. 1 162. F.d. mass spectrum: M^+, vs; $[M - SC_6F_5]^+$, w; $[M - TlSC_6F_5]^+$, vs; $[M - \{Tl(SC_6F_5)_2\}]^+$, w; $[TlSC_6-F_5]^+$, w; and Tl^+, s. Λ 78 Ω^{-1} cm^2 mol^{-1} (10^{-3} mol dm^{-3}). ^{1}H N.m.r. (CD$_2$Cl$_2$, 20 °C): δ 5.55 (s, C$_5$H$_5$).

Red prismatic crystals of (**2**) are obtainable from ethyl acetate–diethyl ether or acetone–diethyl ether.

Reactions of [TlMo(SC$_6$F$_5$)$_2$(CO)$_2$(cp)].—*With* PMe$_2$Ph. Dimethylphenylphosphine (0.17 g, 0.12 mmol) was added to a solution of complex (**1**) (0.10 g, 0.12 mmol) in diethyl ether (30 cm^3) at r.t. After *ca.* 2 min, the resulting cloudy orange solution was filtered, reduced in volume, mixed with hexane (*ca.* 10 cm^3), and cooled to -15 °C. Red crystals of [Mo(SC$_6$F$_5$)(CO)$_2$-(PMe$_2$Ph)(cp)] (**3**) formed, 0.031 g (47%) [Found: C, 45.5; H, 2.8. Calc. for C$_{21}$H$_{16}$F$_5$MoO$_2$PS: C, 45.4; H, 2.9%; M^+ = 554 (^{96}Mo, e.i.m.s.)]. I.r.: ν(CO) 1 955 and 1 874 cm^{-1}. ^{1}H N.m.r. (CDCl$_3$, r.t.): *cis* isomer (relative intensity 31), δ 1.91 (d, 9) and 1.93 (d, 9 Hz) (diastereotopic PCH$_3$), 5.41 (s, C$_5$H$_5$), and 7.41—

7.66 (m, PC_6H_5); *trans* isomer (relative intensity 1), 1.74 (d, 13, PCH_3), 5.04 (d, 2.4 Hz, C_5H_5), and 7.41—7.66 (m, PC_6H_5).

With PMePh$_2$. Methyldiphenylphosphine (0.024 g, 0.12 mmol) was added to complex (1) (0.10 g, 0.12 mmol) in dichloromethane (30 cm^3) at r.t. to give a cloudy orange solution. Filtration of this solution, reduction in volume, addition of hexane, and cooling to $-15\,^{\circ}C$ gave [Mo(SC$_6$F$_5$)-(CO)$_2$(PMePh$_2$)(cp)] (4) as a pink solid (0.037 g, 50%) [Found: C, 50.6; H, 2.8. Calc. for $C_{26}H_{18}F_5MoO_2PS$: C, 50.65; H, 2.9%. M^+ = 616 (^{96}Mo, e.i.m.s.)]. I.r.: ν(CO) 1 955 and 1 878 cm^{-1}. ^{1}H N.m.r. (CDCl$_3$, r.t.): *cis* isomer, δ 2.17 (d, 8.4 Hz, PCH_3), 5.37 (s, C_5H_5), and 7.4 (br m, PC_6H_5).

With PPh$_3$. As above, complex (1) (0.10 g, 0.12 mmol) and PPh$_3$ (0.032 g, 0.12 mmol) yielded pink crystals of [Mo-(SC$_6$F$_5$)(CO)$_2$(PPh$_3$)(cp)] (5), 0.063 g (77%) [Found: C, 54.7; H, 2.9. Calc. for $C_{31}H_{20}F_5MoO_2PS$: C, 54.9; H, 2.95%. M^+ = 678 (^{96}Mo, e.i.m.s.)]. I.r.: ν(CO) 1 958 and 1 878 cm^{-1}. ^{1}H N.m.r. (CDCl$_3$, r.t.): *cis* isomer (relative intensity 17), δ 5.39 (s, C_5H_5) and 7.45 (br m, PC_6H_5); *trans* isomer (relative intensity 1), 5.11 (d, 2 Hz, C_5H_5) and 7.45 (br m, PC_6H_5).

Reaction of [TlMo(SC$_6$F$_5$)$_4$(cp)] (2) *with* PPh$_3$.—Complex (2) (0.070 g, 0.06 mmol) and triphenylphosphine (0.03 g, 0.11 mmol) were stirred in dichloromethane (30 cm^3) at r.t. for 8 d. The cloudy red solution was filtered, reduced in volume, mixed with hexane (*ca.* 10 cm^3), and cooled to $-15\,^{\circ}C$. The resulting red crystals were recrystallised from dichloromethane–hexane giving pure [TlMo(SC$_6$F$_5$)$_4$(PPh$_3$)$_2$(cp)] (6), 0.015 g (15%) (Found: C, 46.2; H, 2.1; P, 3.6; S, 7.3. Calc. for C_{65}-$H_{35}F_{20}MoP_2S_4Tl$: C, 46.3; H, 2.1; P, 3.7; S, 7.6%). N.m.r.: ^{1}H (CDCl$_3$, r.t.), δ 5.5 (s, C_5H_5) and 7.4—7.7 (m, PC_6H_5); ($C_6D_5CD_3$, phenyl resonances obscured) (20 $^{\circ}$C) 5.3 (s, C_5H_5); ($-40\,^{\circ}C$) isomer (a) (relative intensity 1) 5.1 (d, 5.0 Hz, C_5H_5), isomer (b) (relative intensity 3) 5.4 (s, C_5H_5); ^{31}P-$\{^1$H$\}$ ($C_6D_5CD_3$, $-70\,^{\circ}C$), isomer (a) (relative intensity 1) 35.4 (s, PPh$_3$), isomer (b) (relative intensity 3) 23.0 p.p.m. (s, PPh$_3$).

Crystal Structure Determinations.—Crystal data for complex (1). $C_{19}H_5F_{10}MoO_2S_2Tl$, red prisms, monoclinic, a = 17.210(6), b = 10.598(2), c = 12.109(4) Å, β = 99.86(3)$^{\circ}$, U = 2 176.0 Å^3, Z = 4, D_c = 2.501 g cm^{-3}, $F(000)$ = 1 520, μ(Mo-K_α) = 83.2 cm^{-1}, space group $P2_1/a$ (non-standard $P2_1/c$, no. 14) from systematic absences.

Data collection, structure solution, and refinement. The intensity data from a crystal of complex (1) (*ca.* 0.10 $\times$ 0.145 $\times$ 0.32 mm) were measured on an Enraf-Nonius CAD4 diffractometer using ω—2θ scans and graphite-monochromated Mo-K_α radiation (λ = 0.710 693 Å) over the range 1.0 $< \theta <$ 25°. The 3 818 unique data were corrected for Lorentz and polarisation, and absorption (DIFABS^{26}). The positions of the Tl and Mo atoms were found initially on a Patterson map (SHELXS 86^{27}) with the remainder of the structure being located on subsequent Fourier difference maps. The structure was refined by full-matrix least-squares techniques (SHELX 76^{28}) with anisotropic thermal parameters for all the non-hydrogen atoms. The cyclopentadienyl group was treated as a rigid pentagon (C–C 1.42 and C–H 1.08 Å). At convergence, the discrepancy indices R and R' $\{w = 1/[\sigma^2(F_o) + 0.0016(F_o^2)]\}$ were 0.051 and 0.058 respectively for 2 210 reflections with $I > 2\sigma(I)$, where σ is the standard deviation in the background count based on counting statistics. The final Fourier difference map exhibited two features of *ca.* 0.9 e Å^{-3} in the vicinity of the thallium atom, with a general noise level of less than ± 0.5 e Å^{-3}.

Crystal data for complex (2). $C_{29}H_5F_{20}MoS_4Tl$, orange-red plates, orthorhombic, a = 14.388(4), b = 14.841(4), c = 14.904(4) Å, U = 3 182.5 Å^3, Z = 4, D_c = 2.675 g cm^{-3}, $F(000)$ = 2 424, μ(Mo-K_α) = 59.0 cm^{-1}.

Data collection, structure solution, and refinement. The X-ray intensity data from a small orange-red crystal of complex (2) (*ca.* 0.2 $\times$ 0.25 $\times$ 0.10 mm) were collected as described above for (1) over the range 1.0 $< \theta <$ 28°. Corrections for Lorentz and polarisation and absorption (DIFABS^{26}) were applied to the 3 971 unique data measured. Although the systematic absences were consistent with either of the space groups *Pnma* (no. 63) or *Pn2$_1$a* (non-standard setting of no. 33), the latter was found to be correct from successful structure solution and refinement (see below). The structure was solvent by careful application of Patterson (Tl and Mo atoms) and Fourier difference (S, F, and C atoms) methods. Subsequent structural refinement was carried out using full-matrix least-squares methods (GX^{29}) with anisotropic thermal parameters for the Tl, Mo, and S atoms. The pentafluorophenyl (C–C 1.375 and C–F 1.34 Å) and cyclopentadienyl (C–C 1.42 and C–H 1.08 Å) substituents were treated as idealised rigid groups. The final conventional and weighted [$w = 1/\sigma^2(F)$] R factors were 0.052 and 0.050 respectively for 1 472 data with $I > 3\sigma(I)$. The final Fourier difference map contained six peaks in the range ± 0.9—1.1 e Å^{-3} close to the Tl and Mo atoms, with a background level of less than ± 0.6 e Å^{-3}.

Structural diagrams were plotted with the aid of ORTEP^{30} and PLUTO.^{31}

Additional material available from the Cambridge Crystallographic Data Centre comprises H-atom co-ordinates and thermal parameters.

Acknowledgements

References

1 P. J. Blower and J. R. Dilworth, *Coord. Chem. Rev.*, 1987, **76**, 121 and refs. therein.

2 P. M. Treichel and P. C. Nakagaki, *Organometallics*, 1986, **5**, 711 and refs. therein.

3 R. Havlin and G. R. Knox, *Z. Naturforsch., Teil B*, 1966, **21**, 1108; P. S. Braterman, J. L. Davidson, and D. W. A. Sharp, *J. Chem. Soc., Dalton Trans.*, 1976, 241.

4 J. L. Davidson, *J. Chem. Soc., Dalton Trans.*, 1986, 2423; J. L. Davidson, M. Green, F. G. A. Stone, and A. J. Welch, *ibid.*, 1977, 287.

5 M. T. Ashby and J. H. Enemark, *J. Am. Chem. Soc.*, 1986, **108**, 730.

6 J. L. Davidson, K. Davidson, W. E. Lindsell, N. W. Murrall, and A. J. Welch, *J. Chem. Soc., Dalton Trans.*, 1986, 1677.

7 I. B. Benson, S. D. Killops, S. A. R. Knox, and A. J. Welch, *J. Am. Chem. Soc., Chem. Commun.*, 1980, 1137.

8 J. Courtot-Coupez, M. Guéguen, J. E. Guerchais, F. Y. Petillon, J. Talarmin, and R. Mercier, *J. Organomet. Chem.*, 1986, **312**, 81.

9 R. B. King, *J. Am. Chem. Soc.*, 1963, **85**, 1587; N. G. Connelly and L. F. Dahl, *ibid.*, 1970, **92**, 7470; M. Rakowski-Dubois, R. C. Haltiwanger, D. J. Miller, and G. Glatzmaier, *ibid.*, 1979, **101**, 5245.

10 C. J. Casewit, W. K. Miller, D. E. Coons, L. L. Wright, and M. Rakowski-Dubois, *Organometallics*, 1986, **5**, 591 and refs. therein.

11 F. Y. Pettillon, J. L. Le Quere, J. Roue, J. E. Guerchais, and D. W. A. Sharp, *J. Organomet. Chem.*, 1980, **204**, 207.

12 J. Courtot-Coupez, J. E. Guerchais, F. Y. Petillon, and J. Talarmin, *J. Chem. Soc., Dalton Trans.*, 1986, 1917; J. E. Guerchais, J. L. Le Quere, F. Y. Petillon, L. Manojlovic-Muir, and D. W. A. Sharp, *ibid.*, 1982, 283.

13 (*a*) W. A. W. A. Bakar, J. L. Davidson, W. E. Lindsell, K. J. McCullough, and K. W. Muir, *J. Organomet. Chem.*, 1987, **322**, C1; (*b*) J. L. Davidson, K. Davidson, and W. E. Lindsell, *J. Chem. Soc., Chem. Commun.*, 1983, 4452.

14 *Cf.* S. Bianca, *Rev. Roum. Chim.*, 1975, **20**, 473.

15 See, for example, K. W. Barnet and D. W. Slocum, *J. Organomet. Chem.*, 1972, **44**, 1; J. W. Faller and A. S. Anderson, *J. Am. Chem. Soc.*, 1970, **92**, 5852.

16 J. Rajaram and J. A. Ibers, *Inorg. Chem.*, 1973, **12**, 1313.

17 S. Wang, J. P. Fackler, C. King, and J. C. Wang, *J. Am. Chem. Soc.*, 1988, **110**, 3308 and refs. therein.

18 (*a*) H. Pritzkow and P. Jennische, *Acta Chem. Scand., Ser. A*, 1975, **29**, 60; (*b*) P. M. Potel, R. Chevrel, and M. Sergent, *Acta Crystallogr., Sect. B*, 1980, **36**, 1319; (*c*) G. Eulenberger, *ibid., Sect. C*, 1986, **42**, 528; (*d*) R. W. Alkire, A. C. Larson, P. J. Vergamini, and B. Morosin, *ibid.*, 1985, **41**, 1709.

19 R. Uson, J. Forniés, M. Thomas, and J. H. Cassas, *J. Am. Chem. Soc.*, 1985, **107**, 2556.

20 *cf.* P. I. Van Vliet and K. Vrieze, *J. Organomet. Chem.*, 1977, **139**, 337.

21 D. Kost, E. H. Carlson, and M. Raban, *Chem. Commun.*, 1971, 656.

22 W. A. W. A. Bakar, J. L. Davidson, W. E. Lindsell, and K. J. McCullough, *J. Chem. Soc., Dalton Trans.*, submitted for publication.

23 C. White and R. J. Mawby, *Inorg. Chim. Acta*, 1970, **4**, 261.

24 J. L. Davidson and G. Vasapollo, *J. Organomet. Chem.*, 1985, **291**, 43.

25 J. L. Davidson and D. W. A. Sharp, *J. Chem. Soc., Dalton Trans.*, 1975, 2531.

26 N. G. Walker and D. Stuart, *Acta Crystallogr., Sect. A*, 1983, **39**, 158.

27 G. M. Sheldrick, SHELXS 86, University of Göttingen, Germany, 1986.

28 G. M. Sheldrick, SHELX 76, University of Cambridge, 1976.

29 P. R. Mallinson and K. Muir, *J. Appl. Crystallogr.*, 1985, **18**, 51.

30 C. K. Johnson, ORTEP, Report ORNL-5183, Oak Ridge National Laboratory, Tennessee, 1976.

31 W. D. S. Motherwell, PLUTO, University of Cambridge, 1976.